Comparative experimental and modeling studies of the viscosity behavior of ethanol + C7 hydrocarbon mixtures versus pressure and temperature

Claus K. Zéberg-Mikkelsen[1], Guillaume Watson[2], Antoine Baylaucq[2], Guillaume Galliéro[2], Christian Boned[2*]

[1] Center for Phase Equilibria and Separation Processes, Department of Chemical Engineering, Technical University of Denmark, Building 229, 2800 Lyngby, Denmark

[2] Laboratoire des Fluides Complexes, Faculté des Sciences et Techniques, UMR CNRS 5150, Université de Pau, BP 1155, 64013 Pau Cedex, France

[*] Corresponding author. Phone: (+33) 5 59 40 76 88; Fax: (+33) 5 59 40 76 95; E-mail: christian.boned@univ-pau.fr

Abstract

The viscosity of the binary system ethanol + n-heptane has been measured with a falling-body viscometer for seven compositions as well as for the pure compounds in the temperature range (293.15 to 353.15) K and up to 100 MPa with an experimental uncertainty of 2%. At 0.1 MPa the viscosity has been measured with a classical capillary viscometer (Ubbelohde) with an uncertainty of 1%. A total of 208 experimental measurements are reported for this binary system. The viscosity behavior of this binary system is interpreted as the results of changes in the free volume, and the breaking or weakening of hydrogen bonds. The excess activation energy for viscous flow of the mixtures is negative with a maximum absolute value of 0.3 $kJ \cdot mol^{-1}$, indicating a very weakly interacting system and showing a negative departure from ideality. The data of this binary system as well as those recently measured for ethanol + toluene have been used in a study of the performance of some viscosity models with a physical and theoretical background. The evaluated models are based on the hard-sphere scheme, the concepts of the free-volume and the friction theory, and a model derived from molecular dynamics. In addition to these models, the simple mixing laws of Grunberg-Nissan and Katti-Chaudhri are also applied in the representation of the viscosity behavior of these ethanol + C_7 hydrocarbon systems. Overall a satisfactory representation of the viscosity of these two binary systems is found for the different models within the considered *T,P* range taken into account their simplicity.

Key Words: *ethanol, high pressure, hydrocarbon, measurements, modeling, viscosity.*

1. Introduction

In order to study and understand the behavior of alcohol + hydrocarbon or petroleum systems under various operating conditions, their thermophysical properties are needed. Since these fluids may be multicomponent mixtures involving paraffinic, naphthenic, and aromatic compounds as well as alcohols, it is impossible to experimentally determine all their properties at all temperature, pressure, and composition (T,P,x) conditions. As a consequence, different property models are required in order to describe the behavior of these fluids. However, experimental property studies of simplified mixtures can provide valuable information about their behavior under various T,P,x conditions from both a fundamental and an applied point of view.

In this work, the focus is addressed to mixtures involving ethanol and hydrocarbons. Ethanol is used in many industrial applications, such as solvent in paints or pharmaceuticals, in the manufacturing of acetic acid, ether, or high-molecular weight chemicals etc. In the last years, ethanol has become of great interest as an additive to gasoline instead of the commonly used compound methyl tert-butyl ether (MTBE), which is found to have some environmental damaging side effects, e.g. to penetrate through the soil, entering into and polluting the ground water. Consequently, ethanol is now e.g. in the USA, added to gasoline (gasohol). As discussed by French and Malone [1], the addition of ethanol to gasoline affects the production, storage, distribution, and use of the obtained gasoline, because the physical properties are changed and complex thermodynamic behaviors are encountered.

Although the viscosity is an important fluid property, which is required in a wide range of engineering disciplines, only a few experimental studies have previously

been performed for alcohol + hydrocarbon systems under pressure [2,3]. Due to the lack of high-pressure viscosity measurements, an extensive experimental study is initiated on binary systems composed of ethanol and C_7 hydrocarbons in order to provide experimental data and to study the influence on the viscosity behavior related to different chemical families. Recently, the viscosity has been measured for ethanol + toluene [4], revealing a complex behavior involving a minimum in the behavior of viscosity versus composition, which is interpreted as the result of differences in the molecular structure, changes in the free volume, and molecular interactions. In this work, the viscosity is measured for ethanol + n-heptane over the entire composition range, up to 100 MPa and in the temperature range 293.15 – 353.15 K using a falling-body viscometer. These data as well as those recently measured for ethanol + toluene [4] are used in a study of the performance of some viscosity models with a physical and theoretical background. The evaluated models are based on the hard-sphere scheme [5,6], the concepts of the free-volume [7,8] and the friction theory [9,10], and a model derived from molecular dynamics simulations [11]. In addition to these models, the simple mixing laws of Grunberg and Nissan [12] and Katti and Chaudhri [13] are also applied in the representation of the viscosity behavior of these ethanol + C_7 hydrocarbon systems.

2. Experimental Techniques

The dynamic viscosity η was measured under pressure using a falling-body viscometer of the type designed by Daugé et al. [14] in order to measure the liquid and dense phase viscosity of fluids with a low viscosity, and which are not in the single liquid phase at atmospheric pressure. A detailed technical description of the viscometer

is given in Ref. 14. The pressure within the viscometer is measured by a HBM-P3M manometer with an uncertainty of 0.1 MPa. The temperature is measured inside the viscometer by a Pt100 probe connected to a classical AOIP thermometer with an uncertainty of 0.5 K. The temperature of the sample in the viscometer is controlled by a circulating fluid. Further, the viscometer is placed in an automated air-pulsed thermal regulator box in order to ensure a homogeneous temperature surrounding the viscometer. In the case of fluids, which are liquid at atmospheric pressure, the filling procedure of the viscometer is simplified compared to the procedure described in [14].

The basic principle of the falling-body viscometer is that a sinker falls through a fluid of unknown viscosity under a given *T,P* condition. It has been underlined by Daugé et al. [14] that for this type of viscometer and for fluids with a low viscosity a working equation of the functional form: $\eta(T,P) = f[(\rho_S - \rho_L)\,\Delta\tau]$ should be used. This working equation relates the dynamic viscosity to the difference between the density of the sinker ρ_S and of the fluid ρ_L, and the falling time between two detection sensors $\Delta\tau$, when the velocity of the sinker is constant. For fluids with very low viscosity such as methane, Daugé et al. [14] used a second order polynomial in $(\rho_S - \rho_L)\Delta\tau$, which implies the requirement of three reference fluids in order to perform the calibration of the viscometer. Since the viscosity in this work is higher than 0.2 mPa.s, it was found suitable to use a linear relation for the working equation as follows

$$\eta(T,P) = K_a(T,P) + K_b(T,P)(\rho_S - \rho_L)\Delta\tau \qquad (1)$$

which relates the dynamic viscosity to two apparatus constants K_a and K_b. A similar working equation has recently been used [4,15]. The calibration of the viscometer was performed with toluene and n-decane at each *T,P* condition of interest. A detailed

description of the calibration procedure and the used reference viscosities and densities of the calibrating fluids is given in [4]. Since the density of the used stainless steel sinker (ρ_s = 7720 kg·m^{-3}) is about 9 times higher than the density of the fluids considered in this work, an error in the fluid density of 0.1% results in an error around 1/7000 in the dynamic viscosity. Further, in this work, $\Delta\tau$ corresponds to the average value of six measurements of the falling time at thermal and mechanical equilibrium with a reproducibility of 0.5%. The overall uncertainty for the reported dynamic viscosities is of the order of 2%, found at the highest pressure, when taking into account the uncertainty due to the calibration, the temperature, the pressure, and the density.

In this work, the densities of ethanol, n-heptane, and their binary mixtures are taken from [16], where they have been measured up to 65 MPa and in the temperature range (293.15 to 333.15) K for the same compositions considered in this work. The uncertainty reported for these density measurements is 0.1 kg·m^{-3}. The required densities at 353.15 K have been obtained by a linearly extrapolation within an estimated uncertainty lower or equal to 1 kg·m^{-3}. For pressures above 65 MPa, the required densities have been obtained by an extrapolation of the experimental densities using the Tait type relation described in [17].

At atmospheric pressure (0.1 MPa) the dynamic viscosity has been obtained by measuring the kinematic viscosity with a classical capillary viscometer (Ubbelohde). For this purpose several tubes connected to an automatic AVS350 Schott Geräte Analyzer has been used. The temperature of the fluid is controlled within 0.1 K using a thermostatic bath. When multiplying the kinematic viscosity with the density, the dynamic viscosity is obtained with an uncertainty less than 1%.

The compounds used in this study are commercially available chemicals with the following purity levels: ethanol from Riedel-de-Haën with a chemical purity > 99.8 vol% (Gas Chromatography), a water content < 0.2 vol%, and a molecular weight M_w = 46.07 g·mol^{-1}; n-heptane from Riedel-de-Haën with a chemical purity > 99.5% (Gas Chromatography), and a molecular weight M_w = 100.20 g·mol^{-1}; toluene from Aldrich with a chemical purity > 99.8% (HPLC Grade) and M_w = 92.14 g·mol^{-1} and n-decane from Merck with a chemical purity > 99% (Gas Chromatography) and M_w = 142.28 g·mol^{-1}. The pure compounds were used as received and stored in hermetically sealed bottles. The binary ethanol (1) + n-heptane (2) mixtures were prepared immediately before use by weighing at atmospheric pressure and ambient temperature using a high-precision Sartorius balance with an uncertainty of 0.001 g. For each mixture, a sample of 250 g was prepared, which, taking into account the uncertainty of the balance, resulted in an uncertainty in the mole fraction of less than $2 \cdot 10^{-5}$.

3. Results

As a consequence that ethanol is a gas at 353.15 K and 0.1 MPa and in order to ensure that the experimental work is carried out in the single phase liquid region at 0.1 MPa, the vapor liquid equilibrium (VLE) phase diagram at 0.1 MPa is required. Several measurements of the VLE behavior at 0.1 MPa for ethanol + n-heptane are reported in the literature {18-20]. The VLE phase diagram at 0.1 MPa is shown in Figure 1 revealing an azeotropic behavior. In this figure, the experimental data [18-20] are shown along with the predicted VLE behavior by the PC SAFT equation [21,22] using k_{ij} = 0.0435. A bubble temperature calculation reveals that the overall average absolute deviation (AAD) between the reported temperatures [18-20] and the calculated

values in Kelvin is 0.2 %, whereas the AAD between the experimental vapor mole fraction of ethanol [18-20] and the predicted values is 6.9 %.

Based on the VLE phase diagram, no measurements of the dynamic viscosity were performed at 353.15 K and 0.1 MPa for ethanol as well as the considered binary ethanol + n-heptane mixtures. The measured dynamic viscosities of ethanol, n-heptane and seven of their binary mixtures in the temperature range (293.15 to 353.15) K at each 20 K and for pressures up to 100 MPa in steps of 20 MPa are given in Table 1 as a function of temperature T, pressure P and mole fraction of ethanol x_1.

The measured n-heptane viscosities have been compared with literature values [15,23-29], which are available up to 100 MPa in the temperature range (293.15 to 353.15) K. Some of the literature data have been interpolated in order to obtain values corresponding to the pressures considered in this experimental work. Figure 2 shows the deviations obtained for n-heptane viscosities measured in this work as well as the interpolated literature values [15,23-29], when these viscosity data are compared with the average value obtained by fitting all available viscosity values at the corresponding isobar as a function of the temperature. This figure shows a very good agreement between the n-heptane viscosities of this work and those reported in the literature [15,23-29]. For ethanol, a similar comparison has been performed [4] showing a very good agreement between the experimental ethanol viscosities and those reported in the literature.

For all the mixtures the viscosity increases with increasing pressure and decreasing temperature. Within the considered T,P range, ethanol is more viscous than n-heptane. With increasing temperature the viscosity of ethanol decreases more rapidly than for n-heptane, see Table 1 and Figures 3 and 4. As mentioned in [4], a quantitative

explanation for more rapidly decrease of the viscosity of ethanol with increasing temperature may be due to the weakening or breaking of the formed intermolecular hydrogen bonds (self-association). In Figures 3 and 4 the variation of the viscosity versus concentration is shown for various isobars at 293.15 K and 333.15 K, respectively. At 333.15 K and 353.15 K Table 1 seems to show the presence of a minimum but the variations are within the experimental uncertainty of the viscosity. Consequently, at a given *T,P* condition the viscosity increases monotonically with increasing ethanol concentration. The viscosity behavior of this binary system as a function of the mole fraction shows a negative departure from ideality. This can be explained as the result of the occurring of a volume expansion, when the two pure compounds are mixed, due to disruption of the ordered molecular structure within the liquid and a weakening or breaking of the formed hydrogen bonds between ethanol molecules. In [16], based on the behavior of the experimental density data and the discussion with respect to the excess molar volume, isothermal compressibility, and isobaric thermal expansivity, it has been found that a volume expansion occurs for this binary system.

In comparison, the viscosity behavior of ethanol + toluene reveals a non-monotonical behavior involving a minimum, which becomes more pronounced with increasing temperature [4]. The viscosity behavior of this binary system is also interpreted as the result of changes in the free volume, and the breaking or weakening of hydrogen bonds, despite evidence for electron donor-acceptor type of interactions between the π electrons of aromatic hydrocarbons and the hydroxyl group of alcohols [30-33].

The excess activation energy of viscous flow ΔE_a for this binary system can be calculated from the following expression

$$\ln(\eta_{mix}\, v_{mix}) = x_1 \ln(\eta_1\, v_1) + x_2 \ln(\eta_2\, v_2) + \frac{\Delta E_a}{R\,T} \qquad (2)$$

using the measured viscosities in Table 1 and the molar volumes v obtained from the experimental and extrapolated density data [16]. Further, R is the universal gas constant and subscript *mix* refers to the mixture, whereas subscripts 1 and 2 refer to the pure compounds. This relationship for the excess activation energy of viscous flow is theoretically justified by Eyring´s representation of the dynamic viscosity of pure fluid [34]. In addition, the quantity ηv is also obtained from the time correlation expression for shear viscosity [35].

For this binary system, the variation of the excess activation energy of viscous flow at 313.15 K is shown as a function of the composition for various isobars in Figure 5. Within most of the considered *T,P* conditions, the excess activation energy of viscous flow is negative, which corresponds to the fact that the viscosity of the mixtures is reduced compared to that of an ideal mixture, when ethanol and n-heptane are mixed. But at the highest temperatures and highest pressures the excess activation energy of viscous flow becomes positive in the ethanol rich region. Some authors [36-39] have interpreted negative excess activation energy of viscous flow as the result of the breaking-up of the ordered molecular structure present in the pure liquids and the fact that repulsive forces or molecular interactions predominate, but it may also be the result of volume expansion. According to this, a positive value for excess activation energy of viscous flow should then correspond to the interlinking of molecules or the association of bonds within the ordered molecular structure [40]. The numerical values of the

excess activation energy of viscous flow for the ethanol + n-heptane system increase with increasing pressure. An explanation may be that when a fluid is compressed the molecular free volume decreases, resulting in molecular interlinking effects and a reduction in their mobility, which consequently leads to a higher viscosity.

For this binary system, the absolute maximum value of the excess activation energy of viscous flow $|\Delta E_a|$ is 0.3 kJ·mol^{-1}, which corresponds to a weakly interacting system. For ethanol + toluene the absolute maximum value is also around 0.3 kJ·mol^{-1} [4]. Despite evidence for electron donor-acceptor type of interactions between the π electrons of aromatic hydrocarbons and the hydroxyl group of alcohols [30-33], the excess activation energy of viscous flow for ethanol + toluene is negative within the *T,P* range considered in [4]. To compare with these two ethanol + C_7 hydrocarbon systems, a maximum value of 0.7 kJ·mol^{-1} is found for the binary system methylcyclohexane + 2,2,4,4,6,8,8-heptamethylnonane [40], whereas for very associative systems, such as water + alcohol [41] the maximum numerical value is 5 kJ·mol^{-1}.

4. Models

In order to make a comparative study of the performance of different viscosity models to represent the viscosity of the binary system ethanol + n-heptane as well as the binary system ethanol + toluene [4], the following definitions are used

$$\begin{aligned} \text{Deviation}_\text{i} &= \eta_{\text{calc,i}} / \eta_{\text{exp,i}} - 1 \\ \text{AAD} &= \frac{1}{\text{NP}} \sum_{i=1}^{\text{NP}} \left|\text{Deviation}_\text{i}\right| \\ \text{Bias} &= \frac{1}{\text{NP}} \sum_{i=1}^{\text{NP}} \text{Deviation}_\text{i} \\ \text{MD} &= \text{Maximum}\left|\text{Deviation}_\text{i}\right| \end{aligned} \qquad (3)$$

where NP is the number of data points, η_{exp} the experimental viscosity and η_{calc} the calculated viscosity. The AAD (average absolute deviation) indicates how close the calculated values are to the experimental values, while the quantity Bias is an indication of how well the calculated values are distributed around the experimental values. Further, the quantity MD refers to the absolute maximum deviation.

Further, since some of the considered models require pure component properties, such as the molecular weight or critical properties, these properties have been taken from [42].

4.1. Mixing Laws

Several mixing laws have been developed in order to calculate the viscosity of liquid mixtures. The objective of these mixing laws is to predict the viscosity of liquid mixtures using only the viscosity and molar volume of the pure compounds along with the composition. Two of the most well-known mixing laws for binary systems are

$$\ln(\eta_{mix}) = x_1 \ln(\eta_1) + x_2 \ln(\eta_2) \quad (4)$$

originally proposed by Arrhenius [43], but generally referred to as the "ideal" Grunberg and Nissan mixing law [12], and the one of Katti and Chaudhri [13]

$$\ln(\eta_{mix}\, v_{mix}) = x_1 \ln(\eta_1\, v_1) + x_2 \ln(\eta_2\, v_2) \quad (5)$$

These two viscosity mixing laws are totally predictive in the sense that only pure component properties are required, but are primarily applicable to solutions showing little deviation from ideality [12,13]. In this work, subscript 1 refers to ethanol, whereas subscript 2 refers to the hydrocarbon (either n-heptane or toluene).

In order to calculate the viscosity of the different binary mixtures with Eqs. (4) and (5), the reported viscosities for the pure compounds in this work (Table 1) and in [4] have been used. Further, the required molar volume of the pure compounds and the binary mixtures were estimated from the experimental and extrapolated densities [16, 17, 44]. The obtained deviations between the predicted viscosities and the experimental values are given in Table 2 for both mixing laws. The overall performance for these mixing laws on the two binary systems can be considered satisfactory taking into account the simplicity of the mixing laws. As a result of including the molar volume of the mixtures in the Katti-Chaudhri mixing law additional information about the mixtures is incorporated, and for the two binary systems, the performance of the Katti-Chaudri mixing law is much better than for Grunberg-Nissan. In the Grunberg-Nissan mixing law, the variation of the viscosity versus composition is monotonous and no interactions between the components (deviation from an ideal solution) is taken into account. These interactions do appear for ethanol + toluene [4] as the variation of the viscosity versus composition for this system is not monotonous.

In order to account for the non-ideality in binary systems Grunberg and Nissan [12] introduced the following modification of the Arrhenius type of mixing law

$$\ln(\eta_{mix}) = x_1 \ln(\eta_1) + x_2 \ln(\eta_2) + x_1 x_2 d_{1,2} \qquad (6)$$

and Katti and Chaudhri [13] derived the following mixing law

$$\ln(\eta_{mix}\, v_{mix}) = x_1 \ln(\eta_1\, v_1) + x_2 \ln(\eta_2\, v_2) + \frac{x_1 x_2 W_{1,2}}{RT} \qquad (7)$$

In these equations the binary parameters $d_{1,2}$ and $W_{1,2}$ are adjustable quantities supposed to be more characteristic of the intermolecular interactions between the two components. The modeling of the viscosity of ethanol + n-heptane gives $d_{1,2}$ = -0.6895,

resulting in an AAD = 2.40%, a Bias = 0.09%, and a MD = 6.38% found at 353.15 K, 100 MPa, and 62.5 mol% ethanol. For this binary system the adjustable $W_{1,2}$ = -694.4 J·mol^{-1} is found, resulting in an AAD = 2.38%, a Bias = -0.03%, and a MD = 6.47% found at 353.15 K, 100 MPa, and 62.5 mol% ethanol. For ethanol + toluene, the modeling procedure gives $d_{1,2}$ = -0.5971, with an AAD = 1.23%, a Bias = -0.08%, and a MD = 4.20% found at 293.15 K, 100 MPa, and 75 mol% ethanol, whereas for the Katti-Chaudhri mixing law $W_{1,2}$ = -1094 J·mol^{-1}, resulting in an AAD = 1.35%, a Bias = -0.04%, and a MD = 5.09% found at 293.15 K, 100 MPa, and 75 mol% ethanol. These results show that the Grunberg-Nissan and the Katti-Chaudhri mixing laws can model the viscosity for these two asymmetrical binary systems within or close to the experimental uncertainty of 2% when an adjustable parameter is introduced. The two mixing laws give similar results for each of the two binary systems. Further, it can be seen that the four binary interaction parameters are all negative, corresponding to a negative departure from ideality and a lower viscosity.

4.2 The Hard-Sphere Scheme

This scheme [5,6] has been introduced for the simultaneous correlation of the self-diffusion, the viscosity, and the thermal conductivity of dense fluids over wide ranges of pressure and temperature. In this scheme, the transport properties of real dense fluids, expressed in terms of the reduced molar volume $v_r = v/v_0$ with v the molar volume and v_0 the hard-core molar volume, are assumed to be proportional to the exact hard-sphere values. For each reduced transport property universal curves have been determined as a function of v_r [6]. In this work, only the hard-sphere scheme introduced for viscosity estimation is described.

For rough spherical molecules at high densities, Chandler [45] showed that the self-diffusion coefficient and the viscosity could be related to the smooth hard-sphere values of the transport properties. This idea was extended in [5,6] by assuming that a corresponding states relationship exists between the experimental transport properties of rough non-spherical molecules and the smooth hard-sphere values (subscript *shs*). Since the experimental viscosity is proportional to the exact hard-sphere value, the following relation can be defined

$$\eta_{exp} = R_\eta \eta_{shs} \tag{8}$$

where the proportionality factor R_η is the roughness factor, which accounts for the roughness and non-spherical shape of the molecule.

In order to avoid the direct calculation of the viscosity, Dymond [46] found it convenient to express the viscosity as reduced quantities. Based on this, Dymond and Awan [5] derived the following expression relating the reduced smooth hard-sphere viscosity η^*_{shs} to the experimental value η_{exp}

$$\eta^*_{shs} = \frac{\eta^*_{exp}}{R_\eta} = 6.035 \cdot 10^8 \left[\frac{1}{M_w R T}\right]^{1/2} \frac{\eta_{exp} v^{2/3}}{R_\eta} \tag{9}$$

where η^*_{shs} can be obtained from the following empirical expression

$$\log_{10}\left[\eta^*_{shs}\right] = \log_{10}\left[\frac{\eta^*_{exp}}{R_\eta}\right] = \sum_{k=0}^{7} a_{\eta,k} \left(1/v_r\right)^k \tag{10}$$

which was first derived for n-alkanes [6], but later applied to aromatic hydrocarbons [47], alcohols [48], and refrigerants [49]. The $a_{\eta,i}$ coefficients are universal, independent of the chemical structure of the compound and are given in [10].

For various pure compounds it has been observed that v_0 is temperature dependent whereas R_η is temperature independent for pseudo-spherical molecules, such as n-alkanes, but shows a temperature dependency for molecules that either depart too much from sphericity or have hydrogen bonds, such as alcohols [48].

In this work the general expressions for R_η and v_0 have been used for n-heptane [6], toluene [47], and ethanol [48]. The predicted viscosities for the three pure compounds have been compared with the experimental values reported in Table 1 and [4]. The required molar volumes were obtained from the reported densities in [16,44] and the extrapolated density data. The obtained AAD, Bias and MD for the pure compounds are reported in Table 3, revealing a good agreement between the predicted viscosities and the experimental values.

In order to apply the hard-sphere scheme to mixtures, and since the considered binary systems in this work are highly asymmetrical, it was found appropriate to modify the mixing rule for v_0 by making it less symmetrical compared with the originally introduced mixing rule by Assael et al. [50]. In this work the following mixing rules have been used

$$v_{0,mix} = \left(\sum_{i=1}^{n} x_i v_{0,i}^{1/3} \right)^3 \quad ; \quad R_{\eta,mix} = \sum_{i=1}^{n} x_i R_{\eta,i} \quad ; \quad M_{w,mix} = \sum_{i=1}^{n} x_i M_{w,i} \qquad (11)$$

The AAD, MD and Bias obtained for each of the two binary systems are given in Table 3. The overall results are satisfactory, taking into account that for mixtures the viscosity estimation is fully predictive and only based on pure compound properties.

4.3 The Free-Volume Model

Based on the free-volume concept, an approach has been proposed in order to model the viscosity of Newtonian fluids in the gaseous and dense states [7,8]. In this approach, the total viscosity η can be separated into a dilute gas viscosity term η_0 and an additional term $\Delta\eta$, in the following way

$$\eta = \eta_0 + \Delta\eta \tag{12}$$

The term $\Delta\eta$ characterizes the passage in the dense state and is connected to the molecular structure via a representation of the free volume fraction. In this model

$$\Delta\eta = \frac{\rho N_a \zeta L^2}{M_w} \tag{13}$$

where N_a is Avogadro's constant, ζ the friction coefficient of a molecule, and L^2 an average characteristic molecular quadratic length. The friction coefficient ζ is related to the mobility of the molecule and to the diffusion process. Moreover, the free volume fraction $f_v = v_f/v$ (with $v_f = v - v_0$, v the specific molecular volume and v_0 the molecular volume of reference or hard core volume) is for a given temperature T defined as

$$f_v = \left(\frac{RT}{E}\right)^{\frac{3}{2}} \tag{14}$$

by assuming that the molecule is in a state in which the molecular potential energy of interaction with its neighbors is E/N_a. Further, it has been assumed [7,8] that $E = E_0 + PM_w/\rho$ where the term $PM_w/\rho = Pv$ is related to the energy necessary to form the vacant vacuums available for the diffusion of the molecules and where $E_0 = \alpha\rho$ is the energy barrier, which the molecule has to exceed in order to diffuse.

Based on the empirical free-volume relation by Doolittle [51], the following expression for the friction coefficient has been proposed [7,8]

$$\zeta = \zeta_0 \exp\left[\frac{B}{f_v}\right] \tag{15}$$

where B is characteristic of the free volume overlap. The quantity ζ_0 has been defined [7,8] as

$$\zeta_0 = \frac{E}{N_a b_f}\sqrt{\frac{M_w}{3RT}} \tag{16}$$

where b_f is the dissipation length of the energy E.

The general expression for the free-volume viscosity model is obtained by combining Eqs.(12) through (16) and is given below

$$\eta = \eta_0 + \ell\left(\frac{\alpha\rho^2 + PM_w}{\sqrt{3RTM_w}}\right)\exp\left[B\left(\frac{\alpha\rho^2 + PM_w}{RT\rho}\right)^{3/2}\right] \tag{17}$$

or

$$\eta = \eta_0 + \rho\ell\sqrt{\frac{RT}{3M_w}} f_v^{-2/3}\exp\left[\frac{B}{f_v}\right] \tag{18}$$

where $\ell = L^2/b_f$ is homogeneous with a characteristic molecular length. This equation involves three physical parameters ℓ, α and B, which are characteristic of the molecule. The unit for the viscosity is [Pa·s], when all other units are kept in SI units. This model has been shown to accurately represent the viscosity behavior of various hydrocarbons over wide ranges of temperature and pressure in the gaseous, liquid and dense states.

The dilute gas viscosity η_0 can be obtained from any appropriate model. In this work, the model by Chung et al. [52] is used, since it is applicable of predicting the dilute gas viscosity of several polar and non-polar fluids within an uncertainty of 1.5%.

By using the experimental viscosity (Table 1 and [4]) and the density values reported in [16,44] and the extrapolated values, the three characteristic parameters in Eq.(17) were determined for n-heptane and ethanol, whereas they have already been determined for toluene [53]. The fitted parameters as well as those for toluene [53] are given in Table 4, whereas Table 5 contains the modeling results, revealing an excellent representation of the viscosity behavior of the pure compounds.

In order to apply the free-volume model to mixtures, Eq.(18) has been used with the following simple mixing rules

$$B_{mix} = \sum_{i=1}^{n} x_i B_i \qquad ; \qquad \ell_{mix} = \sum_{i=1}^{n} x_i \ell_i \tag{19}$$

and where the free-volume fraction of the mixture $f_{v,mix}$ is determined by the following expression

$$f_{v,mix} = \sum_{i=1}^{n} x_i f_{v,i} \tag{20}$$

where the free-volume fractions of the pure compounds $f_{v,i}$ is estimated by Eq.(14) using $E = \alpha\rho + PM_w/\rho$. The dilute gas viscosity of the mixtures has been estimated by the mixing rule proposed by Wilke [54]. This mixing rule is a function of the composition, the molecular weight, and the dilute gas viscosity of the pure compounds.

For the two binary systems, the comparison of the predicted viscosities with the experimental values resulted in the AAD, MD, and Bias reported in Table 5. The obtained results are satisfactory, considering the simple structure of the model, since only three adjustable parameters are needed for each pure compound along with the experimental density of the fluid.

4.4 The Friction Theory

Starting from basic principles of mechanics and thermodynamics, the friction theory (*f-theory*) for viscosity modeling has been introduced [9]. In the *f-theory* the total viscosity can be written as

$$\eta = \eta_0 + \eta_f \tag{21}$$

where η_0 is the dilute gas viscosity and η_f the residual friction contribution. The friction contribution is related to the van der Waals attractive and repulsive pressure terms, p_a and p_r, of an equation of states (EOS), such as the Peng and Robinson (PR) [55] or the Soave-Redlich-Kwong (SRK) [56] EOS. These EOS are commonly used within the oil industry for phase behavior descriptions. Based on this concept, a general *f-theory* model [10] for hydrocarbons has been introduced with 16 universal constants and one adjustable parameter - a "characteristic" critical viscosity η_c. For hydrocarbons with a simple molecular structure it has been shown that the *f-theory* models [9,10] consisting of a linear correlation on p_a and a quadratic correlation on p_r suffices to accurately represent the viscosity over wide ranges of temperature and pressure

$$\eta_f = \kappa_a p_a + \kappa_r p_r + \kappa_{rr} p_r^{\,2} \tag{22}$$

where the friction coefficients κ_r, κ_a, and κ_{rr} are temperature dependent functions. The *f-theory* has also been applied to the viscosity modeling of alcohols [57].

For a *n* component mixture, the friction coefficients κ_r, κ_a, and κ_{rr} are obtained by the following mixing rules [9,10]

$$\kappa_r = \sum_{i=1}^{n} z_i \kappa_{r,i}$$
$$\kappa_a = \sum_{i=1}^{n} z_i \kappa_{a,i} \qquad (23)$$
$$\kappa_{rr} = \sum_{i=1}^{n} z_i \kappa_{rr,i}$$

with

$$z_i = \frac{x_i}{M_{w,i}^{\varepsilon}\, MM} \qquad (24)$$

and

$$MM = \sum_{i=1}^{n} \frac{x_i}{M_{w,i}^{\varepsilon}} \qquad (25)$$

where $\varepsilon = 0.30$. $M_{w,i}$ and x_i are, respectively, the molecular weight and the mole fraction of component *i*.

Since the mixture friction coefficients in Eq.(22) are estimated with mixing rules based on the friction coefficients of the pure components, they can directly be obtained by a combination of different *f-theory* models, provided that the same EOS is used, as shown in [58].

In this work, the general *f-theory* model [10] in conjunction with the PR EOS has been used for n-heptane and toluene along with the characteristic critical viscosity η_c also reported in [10]. For ethanol, the PR *f-theory* model derived in [57] has been used. In the PR EOS the regular van der Waals mixing rules have been used with a binary interaction parameter $k_{i,j}$ = 0.08 optimized against literature VLE data. Thus, it should be mentioned that the representation of the VLE behavior for the two binary systems within the considered temperature range of this work is not as good as that

found with the PC-SAFT equation [19,20]. The required dilute gas viscosity of the pure compounds has been obtained by the Chung et al. model [52], whereas the dilute gas viscosity of the mixtures has been obtained by applying the mixing rule of Wilke [54].

A comparison of the predicted viscosities using this *f-theory* scheme with the experimental values has been carried out, and the resultant deviations are reported in Table 6. The obtained mixture results are satisfactory taking into account that they are obtained in conjunction with a simple cubic EOS.

4.5 Molecular Dynamics Viscosity Model

Recently, a predictive viscosity approach has been introduced for simple pure fluids and mixtures over a wide range of temperature and pressure [11]. This approach is derived from molecular dynamics simulations using a corresponding state scheme, where the Lennard-Jones (LJ) fluid is taken as the reference compound and a one-fluid approximation is applied to mixtures. A simple correlation has been developed in order to reproduce accurately recent molecular dynamics results on the LJ fluid over a large range of thermodynamic states [11]. This correlation has been defined using LJ reduced units for the temperature T^* and the density ρ^*:

$$T^* = \frac{k_B T}{\varepsilon_x} \quad , \quad \rho^* = \frac{N\sigma_x^3}{V} \cong \frac{N_A\,\sigma_x^3}{v} \tag{26}$$

and for the viscosity η^*

$$\eta^*\left(T^*, \rho^*\right) = \eta \frac{\sigma_x^2}{\sqrt{m_x \varepsilon_x}} = \eta \frac{\sigma_x^2}{\sqrt{\frac{M_{w,x}\varepsilon_x}{N_A}}} \tag{27}$$

where k_B is the Boltzman constant, T the temperature, N the number of particle, V the volume of the simulation box, η the dynamic viscosity, and m_x, σ_x and ε_x are the characteristic LJ potential parameters of the studied fluid (respectively mass, length and energy). The mass of the fluid can be related to the molecular weight M_w and Avogadro's constant N_A in the following way: $m_x = M_{w,x}/N_A$. Further, the number of fluid particles N within the volume V of the simulation box can be related to Avogadro's constant N_A and the molar volume of the fluid v in the following way: $N/V = N_A/v$. The dynamic viscosity is obtained in [Pa·s], when all variable and properties are inserted in SI units.

The reduced viscosity has been expressed as a sum of a classical Chapman-Enskog dilute density contribution η_0^* and a residual viscosity contribution $\Delta\eta^*$ [11]:

$$\eta^*\left(T^*,\rho^*\right)=\eta_0^*\left(T^*\right)+\Delta\eta^*\left(T^*,\rho^*\right) \tag{28}$$

The dilute density contribution is defined as:

$$\eta_0^*\left(T^*\right)=0.17629\frac{\left(T^*\right)^{1/2}}{\Omega_v}A_c \tag{29}$$

where A_c = 0.95, and Ω_v is the collision integral. Neufeld et al. [59] have derived expressions for different collision integrals. In [11] the expression for the 12-6 collision integral is used.

The residual viscosity contribution is expressed as:

$$\Delta\eta^*\left(T^*,\rho^*\right)=b_1\left(e^{b_2\rho^*}-1\right)+b_3\left(e^{b_4\rho^*}-1\right)+b_5\left(T^*\right)^{-2}\left(e^{b_6\rho^*}-1\right) \tag{30}$$

where the b_i coefficients have been regressed against molecular dynamics simulations results on the LJ pure fluid [11].

In order to apply this approach to real fluids, the two LJ molecular parameters (σ_{ii}, molecular length and ε_{ii}, energy parameter) that are supposed to represent the real compound, are required. These molecular parameters have been related to the critical temperature T_c in K and the critical molar volume v_c in $m^3 \cdot mol^{-1}$, through:

$$\varepsilon_{ii} = \frac{k_B T_c}{1.2593} \tag{31}$$

$$\sigma_{ii} = \left(0.302 \frac{v_c}{N_A} \right)^{1/3} \tag{32}$$

The unit for ε_{ii} is [J], and for σ_{ii} is [m]. It should be mentioned that Eq. (32) in conjunction with the critical molar volume taken from [42] is only efficient for simple compounds. For more complex molecules, the critical molar volume should be adjusted on viscosity data.

For an *n* component mixture, a one-fluid approximation, the so-called van der Waals one fluid model is used to define the characteristic molecular length σ_x and energy ε_x of the mixture

$$\sigma_x^3 = \sum_i \sum_j x_i x_j \sigma_{ij}^3 \tag{33}$$

$$\varepsilon_x \sigma_x^3 = \sum_i \sum_j x_i x_j \varepsilon_{ij} \sigma_{ij}^3 \tag{34}$$

where σ_{ij} and ε_{ij} are the cross molecular parameters defined as

$$\sigma_{ij} = \left(\frac{\sigma_{ii}^3 + \sigma_{jj}^3}{2} \right)^{1/3} \tag{35}$$

$$\varepsilon_{ij} = \left(\frac{\varepsilon_{ii} \sigma_{ii}^3 + \varepsilon_{jj} \sigma_{jj}^3}{2 \sigma_{ij}^3} \right) \tag{36}$$

The scheme for calculating the viscosity of real fluids is the following. First, it is necessary to calculate ε_{ii} and σ_{ii} with Eqs. (31) and (32), and then to evaluate the reduced LJ temperature T^* and reduced LJ density ρ^*, with Eq. (26). Having these values, using Eqs. (28) through (30), the reduced viscosity η^* is evaluated. Finally the viscosity η is obtained from Eq. (27). Additionally, for mixtures, Eqs. (35-36), are used to define the cross molecular parameters, and then Eqs. (33) and (34) are applied for the calculation of the equivalent "pseudocomponent" representative of the mixture.

This scheme has been applied on the two binary systems ethanol + toluene and ethanol + n-heptane. Since the pure compounds are somewhat complex compared to the LJ fluids, the critical molar volumes required in this viscosity approach have been adjusted against the reported viscosity data (Table 1 and [4]) in order to minimize the maximum deviation. For ethanol, toluene and n-heptane the critical molar volumes are respectively 182.49, 312.37 and 428.64 $cm^3 \cdot mol^{-1}$. The required molar volumes were obtained from the density data provided in [16,44] and from an extrapolation using a Tait relationship [17] for pressure up to 100 MPa.

The viscosity modeling results obtained by optimizing the critical molar volume are given in Table 7 for the three pure compounds. The results obtained for the two non-polar compounds (n-heptane and toluene) are acceptable, but exhibit the weakness of the simple LJ approximation to mimic an associating behavior when applied to an alcohol compound (ethanol). Such results are not surprising as this scheme only requires two parameters per molecule - the critical temperature and the critical molar volume (adjusted). As expected, these two parameters can not embody all the physics needed to catch the variation of the viscosity behavior with thermodynamic conditions in strongly polar systems, deviating highly from LJ fluids.

It is interesting to note that the deviations on pure compound encompass those on both mixtures as shown in Table 7. Hence, this scheme provides a reasonable estimation of the viscosity of these mixtures despite its intrinsic weakness on the ethanol. The overall results can be considered satisfactory compared to the simplicity of this scheme, which needs only one adjusted parameter per compound, the critical molar volume, for pure fluids and nothing else for mixtures.

5. Conclusion

A total of 208 experimental dynamic viscosity measurements is reported for the binary system ethanol + n-heptane covering the entire composition range for temperatures between (293.15 to 353.15) K and up to 100 MPa. At 0.1 MPa the dynamic viscosity was measured by a classical capillary viscometer (Ubbelohde) with an experimental uncertainty of 1%, whereas the viscosity under pressure was measured with a falling-body viscometer with an experimental uncertainty of 2%. The viscosity behavior of this binary system shows a negative departure from ideality, which leads to a negative excess activation energy of viscous flow for this binary system with a maximum absolute value of $|\Delta E_a| = 0.3$ kJ·mol^{-1}, corresponding to a weakly interacting system. The viscosity behavior of this system is interpreted as the result of changes in the free-volume, disruption of the ordered molecular structure, weakening or breaking of hydrogen bonds.

The experimental data for this binary systems as well as those recently measured for ethanol + toluene [4] have been used in order to evaluate the performance of the classical mixing laws as well as models with a physical and theoretical background; the hard-sphere scheme, the viscosity models based on the concept of the free-volume and

the friction theory, and a viscosity model derived from molecular dynamics. This evaluation shows that some simple predictive models can represent the viscosity of the two binary systems within an acceptable and satisfactory uncertainty for industrial applications, although the two binary systems are very asymmetrical. Figure 7 summarizes the deviations obtained between the values predicted by the different models and the experimental viscosities for the binary mixtures composed of ethanol + n-heptane and ethanol + toluene. Further, for comparison purposes Figures 8 and 9 show the deviations obtained with the different models at all *T,P,x* conditions (pure compounds, except for Grunberg-Nissan and Katti-Chaudhri, and the 14 binary mixtures) as a function of temperature and pressure, respectively. These figures do not reveal any important fluctuation in the variation of the obtained deviations by a given model with temperature and pressure. For most of the models the largest deviations are obtained at the lowest temperatures and lowest pressures.

The classical mixing laws and the hard-sphere scheme can only be applied to liquid or dense fluids, whereas the free-volume model, the friction theory, and the molecular dynamics viscosity model are all applicable to gases, liquids, and dense fluids. Because of this, these three models are more suitable for industrial processes involving different phases or phase changes. Moreover, from a fundamental point of view, the hard-sphere scheme, the free-volume model, and the molecular dynamics model provide some insight on the microstructure of these complex systems. However these viscosity models require the knowledge of the variation of the density versus pressure and temperature. This is not the case for the friction theory, which is an advantage for practical applications compared to the other models.

Acknowledgement

Financial funding of C.K. Zéberg-Mikkelsen is provided by a Talent project from the Danish Technical Research Council (STVF) Contract No. 26-03-0063.

List of Symbols

Latin letters

B	characteristic of the free-volume overlap.
b_f	dissipative length.
E	energy.
E_0	barrier energy.
f_v	free-volume fraction.
K_a and K_b	calibrated apparatus constants.
k_B	Boltzmann´s constant.
L^2	average characteristic molecular quadratic length.
$\ell = L^2 / b_f$	characteristic molecular length.
M	mass.
M_w	molecular weight.
N_a	Avogadro's constant.
P	pressure.
p_a	attractive pressure term.
p_r	repulsive pressure term.
R	universal gas constant.
R_η	Roughness factor for viscosity.
T	temperature.
T^*	LJ reduced temperature.
T_c	critical temperature.
V	volume.
v	molar volume.

v_c critical molar volume.

v_0 hard-core volume.

v_f free volume.

v_r reduced molar volume.

x molar composition.

Greek letters

α specific density energy parameter.

ΔE_a excess activation energy of viscous flow.

ε molecular energy.

η dynamic viscosity.

η^* LJ reduced dynamic viscosity.

η_0 dilute gas viscosity.

η_c characteristic critical viscosity.

η_f residual friction term.

κ_a linear attractive friction coefficient.

κ_r linear repulsive friction coefficient.

κ_{rr} quadratic repulsive friction coefficient.

ρ density.

ρ^* LJ reduced density.

σ molecular length.

τ time.

Ω_v collision integral.

ζ free-volume friction coefficient.

References

[1] R. French, P. Malone. Fluid Phase Equilib. 228-229 (2005) 27 – 40.

[2] D. Papaioannou, C. Panayiotou. J. Chem. Eng. Data 39 (1994) 463 – 466.

[3] U. Sulzner, G. Luft. Int. J. Thermophys. 19 (1998) 43 – 69.

[4] C.K. Zéberg-Mikkelsen, A. Baylaucq, G. Watson, C. Boned. (submitted).

[5]. J.H. Dymond, M.A. Awan. Int. J. Thermophys. 10 (1989) 941 – 951.

[6] M.J. Assael, J.H. Dymond, M. Papadaki, P.M. Patterson. Int. J. Thermophys. 13 (1992) 269 – 281.

[7] A. Allal, M. Moha-Ouchane, C. Boned. Phys. Chem. Liq. 39 (2001) 1 – 30.

[8] A. Allal, C. Boned, A. Baylaucq. Phys. Rev. E. 64 (2001) 011203/1 – 10.

[9] S.E. Quiñones-Cisneros, C.K. Zéberg-Mikkelsen, E.H. Stenby. Fluid Phase Equilibr. 169 (2000) 249 – 276.

[10] S.E. Quiñones-Cisneros, C.K. Zéberg-Mikkelsen, E.H. Stenby. Fluid Phase Equilibr. 178 (2001) 1 – 16.

[11] G. Galliéro, C. Boned, A. Baylaucq. Ind. Eng. Chem. Res. (in press 2005)

[12] L. Grunberg, A.H. Nissan. Nature 164 (1949) 799 – 800.

[13] P.K. Katti, M.M. Chaudhri. J. Chem. Eng. Data 9 (1964) 442 – 443.

[14] P. Daugé, A. Baylaucq, L. Marlin, C. Boned, J. Chem. Eng. Data 46 (2001) 823 – 830.

[15] A. S. Pensado, M.J.P. Comuñas, L. Lugo, J. Fernández J .Chem. Eng. Data 50 (2005 849 – 856.

[16] G. Watson, C.K. Zéberg-Mikkelsen, A. Baylaucq, C. Boned. (submitted).

[17] A. Et-Tahir, C. Boned, B. Lagourette, P. Xans, Int. J. Thermophys. 16 (1995) 1309 – 1334.

[18] H.C. van Ness, C.A. Soczek, N.K. Kochar. J. Chem. Eng. Data 12 (1967) 346 - 351.

[19] Q. Wang, G. Chen, S. Han. Ranliaa Huaxue Xuebao 18 (1990) 185 – 191.

[20] L. Ortega, F. Espiau. Ind. Eng. Chem. Res. 42 (2003) 4978 – 4992.

[21] J. Gross, G. Sadowski. Ind. Eng. Chem. Res. 41 (2002) 5510 – 5515.

[22] J. Gross, G. Sadowski. Ind. Eng. Chem. Res. 40 (2001) 1244 – 1260.

[23] N.A. Agaev, I.F. Golubev. Gaz. Promst´ 8(7) (1963) 50 – 53.

[24] E. Kuss, P. Pollmann. Zeit. Phys. Chem. Neue Folge 68 (1969) 205 – 227.

[25] H. Kashiwagi, T. Makita. Int. J. Thermophys. 3 (1981) 289 – 305.

[26] M.J. Assael, M. Papadaki. Int. J. Thermophys. 12 (1991) 801 – 810.

[27] M. Kanti, B. Lagourette, J. Alliez, C. Boned. Fluid Phase Equilib. 65 (1991) 291 – 304.

[28] M.J. Assael, C.P. Oliveira, M. Papadaki, W.A. Wakeham. Int. J. Thermophys. 13 (1992) 593 – 615.

[29] A. Baylaucq, C. Boned, P. Daugé, B. Lagourette. Int. J. Thermophys. 18 (1997) 3 – 23.

[30] L.H. Jones, R.M. Badger. J. Am. Chem. Soc. 73 (1951) 3132 – 3134.

[31] M. Tamres. J. Am. Chem. Soc. 74 (1952) 3375 – 3378.

[32] Y. Ioki, H. Kawana, K. Nishimoto. Bull. Chem. Soc. Jpn. 51 (1978) 963 – 966.

[33] R.L. Brinkley, R.B. Gupta. AIChE J. 47 (2001) 948 – 953.

[34] S. Glasstone, K.J. Laidler, H. Eyring, H. The Theory of Rate Processes, the Kinetics of Chemical Reactions, Viscosity, Diffusion, and Electrochemical Phenomena (McGraw-Hill, New York, 1941).

[35] R. Zwanzig, Ann. Rev. Phys. Chem. 16 (1965) 67 – 99.

[36] E.L. Heric, J.G. Brewer, J. Chem. Eng. Data 22 (1967) 574 – 583.

[37] I.L. Acevedo, M.A. Postigo, M. Katz, Phys. Chem. Liq. 21 (1990) 87 – 95.

[38] R. Bravo, M. Pintos, A. Amigo, Phys. Chem. Liq. 22 (1991) 245 - 253.

[39] P. Cea, C. Lafuente, J.P. Morand, F.M. Royo, J.S. Urieta, Phys. Chem. Liq. 29 (1995) 69 – 77.

[40] C.K. Zéberg-Mikkelsen, M. Barrouhou, A. Baylaucq, C. Boned, High Temp. High Pressure. 34 (2002) 591 – 601.

[41] M. Moha-Ouchane, C. Boned, A. Allal, M. Benseddik, Int. J. Thermophys. 19 (1998) 161 – 189.

[42] B.E. Poling, J.M. Prausnitz, J.P. O'Connel. The properties of Gases and Liquids; McGraw-Hill: New York, 2001

[43] S. Arrhenius. Z. Physik. Chem. 1 (1887) 285 – 298.

[44]. C.K. Zéberg-Mikkelsen, L. Lugo, J. Garcia, J. Fernández, Fluid Phase Equilibr. (in press 2005).

[45] D. Chandler. J. Chem. Phys. 62 (1975) 1358 – 1363.

[46] J.H. Dymond, Proc. 6th Symposium Thermophysical Properties. ASME, New York (1973) 143 – 157.

[47] M.J. Assael, J.H. Dymond, P.M. Patterson. Int. J. Thermophys. 13 (1992) 895 – 905.

[48] M.J. Assael, J.H. Dymond, S.K. Polimatidou. Int. J. Thermophys. 15 (1994) 189 – 201.

[49] M.J. Assael, J.H. Dymond, S.K. Polimatidou. Int. J. Thermophys. 16 (1995) 761 – 772.

[50] M.J. Assael, J.H. Dymond, M. Papadaki, P.M. Patterson. Int. J. Thermophys. 13 (1992) 659 – 669.

[51] A.K. Doolittle. J. Appl. Phys. 22 (1951) 1471 – 1475.

[52] T.-H. Chung, M. Ajlan, L.L. Lee, K.E. Starling, Ind. Eng. Chem. Res. 27 (1988) 671 – 679.

[53] X. Canet. Ph.D. Thesis, Université de Pau, France (2001).

[54] C.R. Wilke. J. Chem. Phys. 18 (1950) 517 – 519.

[55] D.-Y. Peng, D.B. Robinson, Ind. Eng. Chem. Fundam. 15 (1976) 59 – 64.

[56] G.S. Soave, Chem. Eng. Sci. 27 (1972) 1197 – 1203.

[57] C.K. Zéberg-Mikkelsen, S.E. Quiñones-Cisneros, E.H. Stenby. Fluid Phase Equilibr. 194-197 (2002) 1191 – 1203.

[58] C.K. Zéberg-Mikkelsen, S.E. Quiñones-Cisneros, E.H. Stenby. Int. J. Thermophys. 23 (2002) 437 – 454.

[59] P.D. Neufeld, A.R. Janzen, R.A. Aziz. J. J. Chem. Phys. 57 (1972) 1100 – 1102.

Table 1. Experimental dynamic viscosities η for ethanol (1) + n-heptane (2) mixtures versus temperature T, pressure P, and mole fraction x_1.

		$x_1 = 0$	$x_1 = 0.125$	$x_1 = 0.250$	$x_1 = 0.375$	$x_1 = 0.500$	$x_1 = 0.625$
T / K	P / MPa	η / mPa·s					
293.15	0.1	0.410	0.419	0.450	0.494	0.556	0.644
293.15	20	0.509	0.518	0.547	0.597	0.668	0.760
293.15	40	0.604	0.614	0.648	0.707	0.787	0.888
293.15	60	0.706	0.718	0.757	0.824	0.913	1.022
293.15	80	0.817	0.832	0.875	0.951	1.047	1.162
293.15	100	0.937	0.953	1.003	1.087	1.191	1.312
313.15	0.1	0.333	0.336	0.354	0.383	0.421	0.475
313.15	20	0.408	0.413	0.429	0.464	0.508	0.567
313.15	40	0.487	0.495	0.513	0.553	0.602	0.666
313.15	60	0.570	0.579	0.599	0.644	0.699	0.768
313.15	80	0.658	0.666	0.690	0.739	0.800	0.874
313.15	100	0.751	0.758	0.786	0.838	0.906	0.984
333.15	0.1	0.276	0.274	0.282	0.299	0.325	0.361
333.15	20	0.336	0.332	0.344	0.364	0.393	0.435
333.15	40	0.402	0.400	0.414	0.436	0.469	0.515
333.15	60	0.472	0.471	0.486	0.511	0.546	0.595
333.15	80	0.546	0.544	0.560	0.589	0.623	0.677
333.15	100	0.623	0.621	0.636	0.670	0.703	0.761
353.15	0.1	0.232					
353.15	20	0.289	0.282	0.286	0.298	0.316	0.341
353.15	40	0.346	0.337	0.343	0.357	0.376	0.403
353.15	60	0.401	0.394	0.401	0.412	0.434	0.464
353.15	80	0.458	0.450	0.458	0.475	0.499	0.530
353.15	100	0.521	0.513	0.522	0.539	0.565	0.599

Table 1. *Continue.*

		$x_1 = 0.750$	$x_1 = 0.875$	$x_1 = 1$
T / K	P / MPa		η / mPa·s	
293.15	0.1	0.757	0.931	1.194
293.15	20	0.885	1.052	1.344
293.15	40	1.023	1.200	1.494
293.15	60	1.168	1.354	1.647
293.15	80	1.316	1.509	1.797
293.15	100	1.473	1.674	1.955
313.15	0.1	0.550	0.660	0.826
313.15	20	0.650	0.766	0.948
313.15	40	0.756	0.877	1.059
313.15	60	0.864	0.989	1.171
313.15	80	0.974	1.102	1.282
313.15	100	1.088	1.217	1.392
333.15	0.1	0.409	0.484	0.590
333.15	20	0.489	0.565	0.683
333.15	40	0.571	0.651	0.769
333.15	60	0.653	0.734	0.851
333.15	80	0.735	0.816	0.934
333.15	100	0.818	0.898	1.015
353.15	0.1			
353.15	20	0.374	0.423	0.510
353.15	40	0.437	0.490	0.574
353.15	60	0.501	0.556	0.636
353.15	80	0.565	0.622	0.699
353.15	100	0.631	0.690	0.763

Table 2. Results for viscosity predictions with the classical ideal mixing laws.

	NP	AAD%	MD%	Bias%
Grunberg-Nissan				
Ethanol + n-Heptane	161	14.0	25.8	14.0
Ethanol + Toluene	161	11.8	18.6	11.8
Katti-Chaudhri				
Ethanol + n-Heptane	161	5.04	13.1	4.98
Ethanol + Toluene	161	7.98	13.7	7.98

Table 3. Results for viscosity predictions with the hard-sphere scheme.

	NP	AAD%	MD%	Bias%
Ethanol	23	2.73	6.22	-1.69
n-Heptane	24	2.55	7.62	-0.28
Toluene	24	1.34	2.13	-1.31
Ethanol + n-Heptane	161	8.77	22.6	-6.68
Ethanol + Toluene	161	10.2	31.3	9.87

Table 4. Characteristic parameters for pure compounds used in the free-volume model.

	α [J m^3·mole^{-1}·kg^{-1}]	B	l [Å]
Ethanol	322.363	0.00219443	0.103238
n-Heptane	101.515	0.00710039	0.796475
Toluene [52]	75.6836	0.00925373	0.727323

Table 5. Results for viscosity predictions with the free-volume viscosity model.

	NP	AAD%	MD%	Bias%
Ethanol	23	0.83	1.43	-0.01
n-Heptane	24	0.60	2.66	0.00
Toluene	24	0.67	1.70	0.05
Ethanol + n-Heptane	161	6.39	23.0	-5.18
Ethanol + Toluene	161	7.04	24.4	-5.34

Table 6. Results for viscosity predictions with the friction theory using the PR EOS.

	NP	AAD%	MD%	Bias%
Ethanol	23	1.97	3.23	-1.11
n-Heptane	24	1.54	3.40	1.33
Toluene	24	2.60	8.22	-1.96
Ethanol + n-Heptane	161	4.92	12.7	4.92
Ethanol + Toluene	161	5.31	11.0	5.30

Table 7. Results for viscosity predictions with a LJ molecular dynamics derived viscosity model.

	NP	AAD%	MD%	Bias%
Ethanol	23	11.4	24.3	-1.24
n-Heptane	24	3.96	8.46	-0.78
Toluene	24	2.61	4.67	0.25
Ethanol + n-Heptane	161	5.16	22.5	0.12
Ethanol + Toluene	161	7.75	22.9	-6.50

Figure 1.

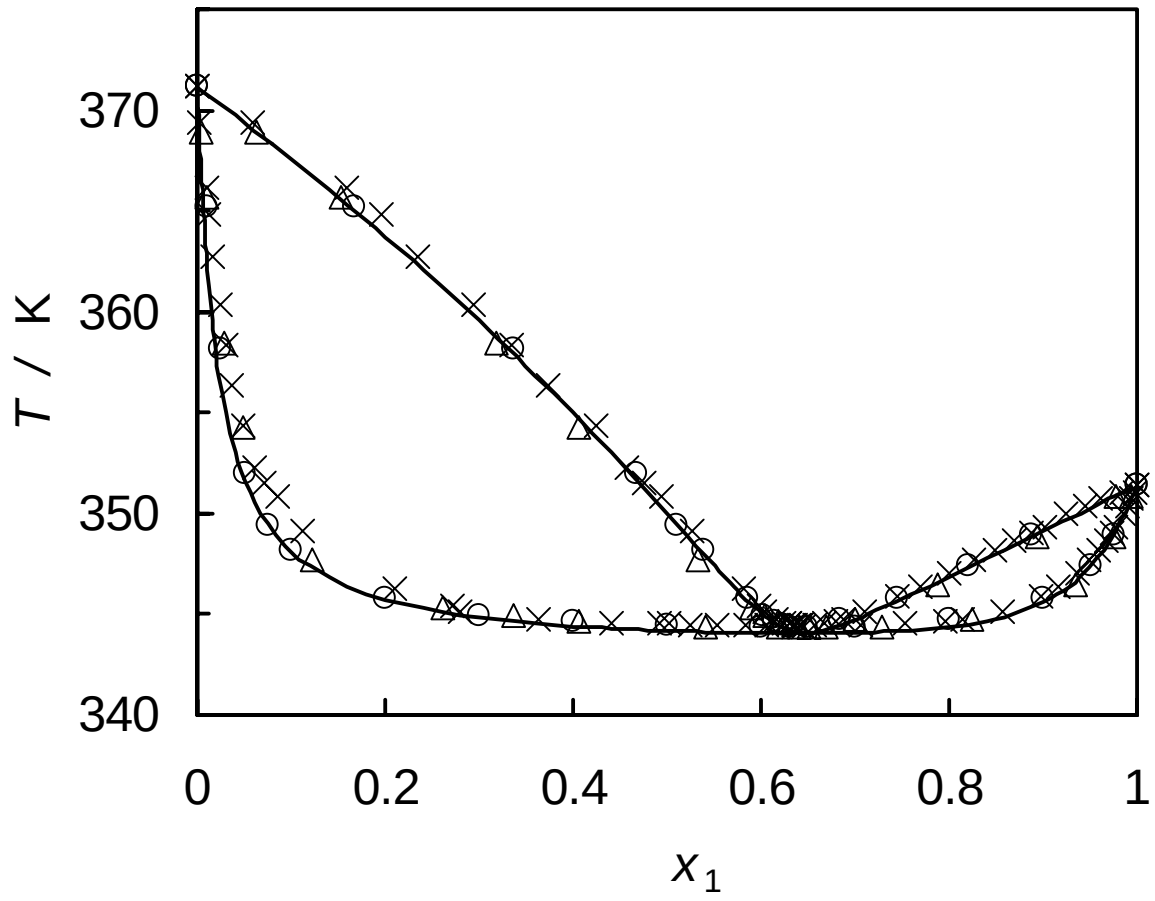

Figure 2.

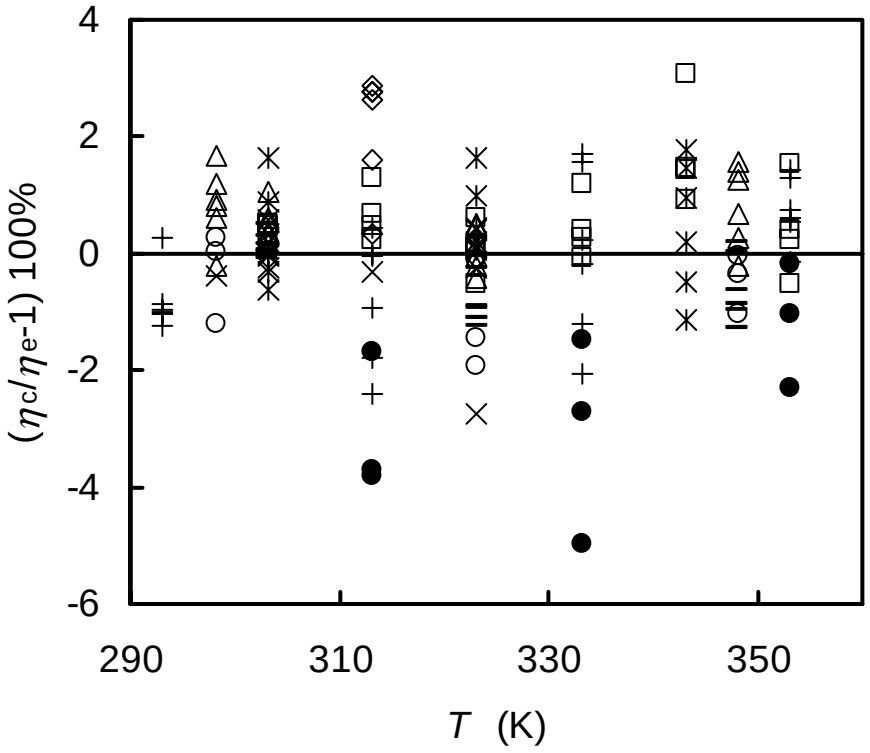

Figure 3.

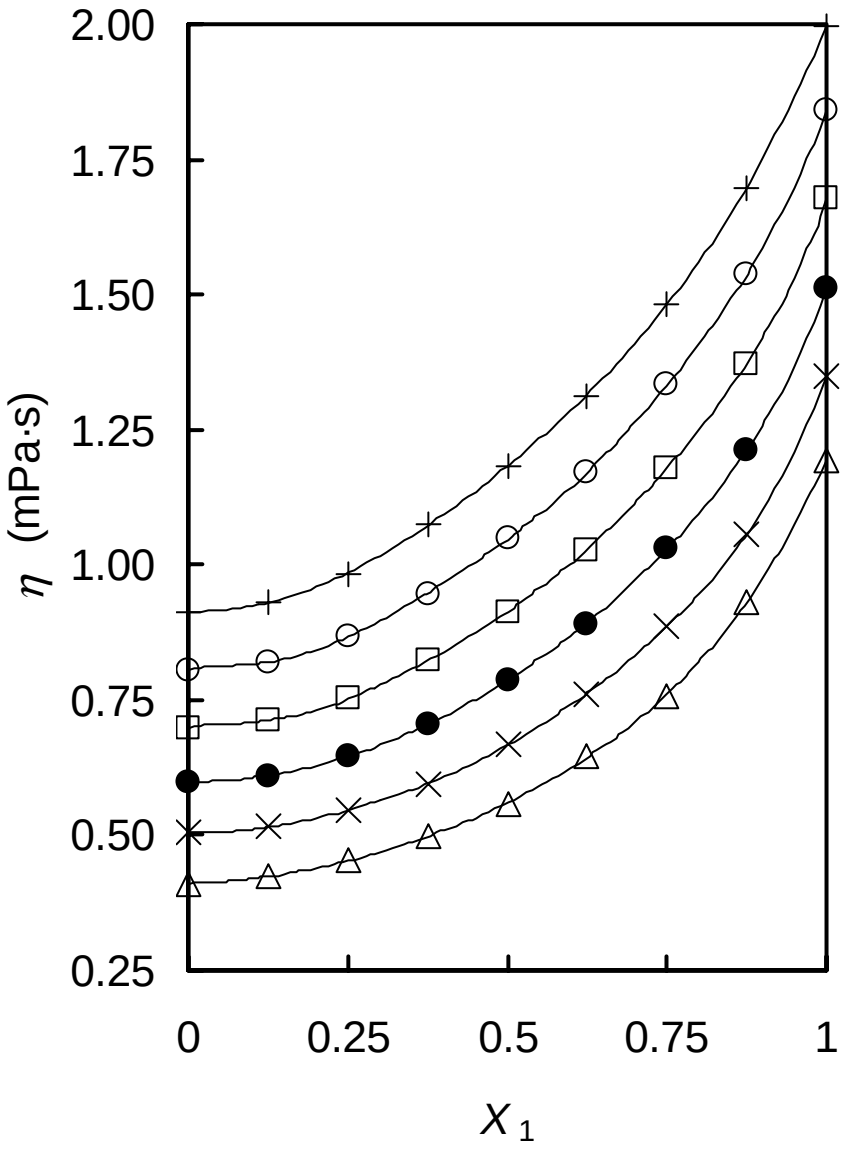

Figure 4.

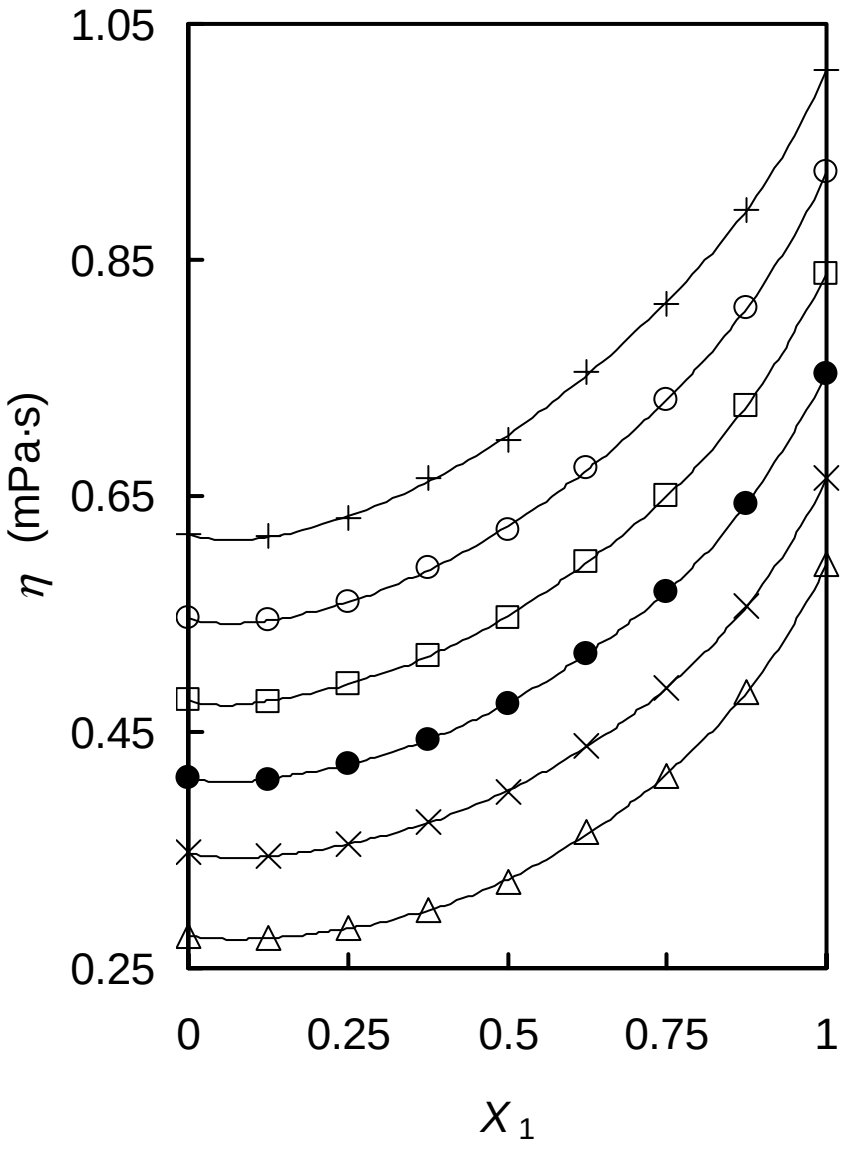

Figure 5.

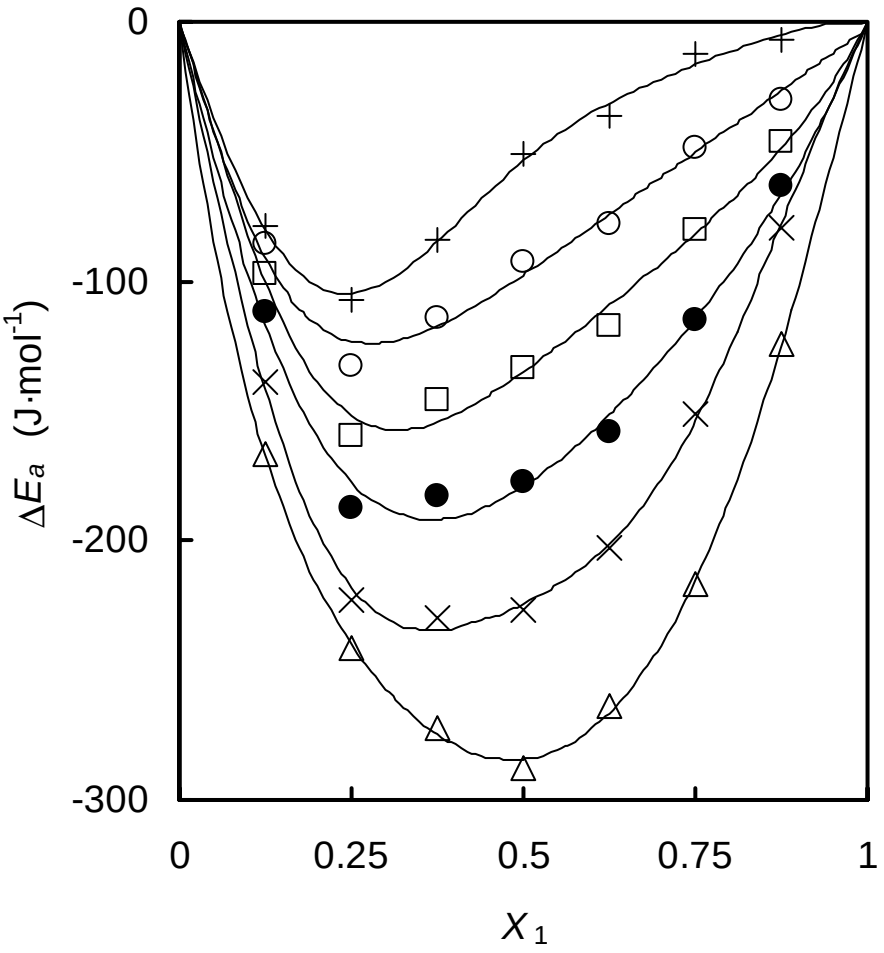

Figure 6.

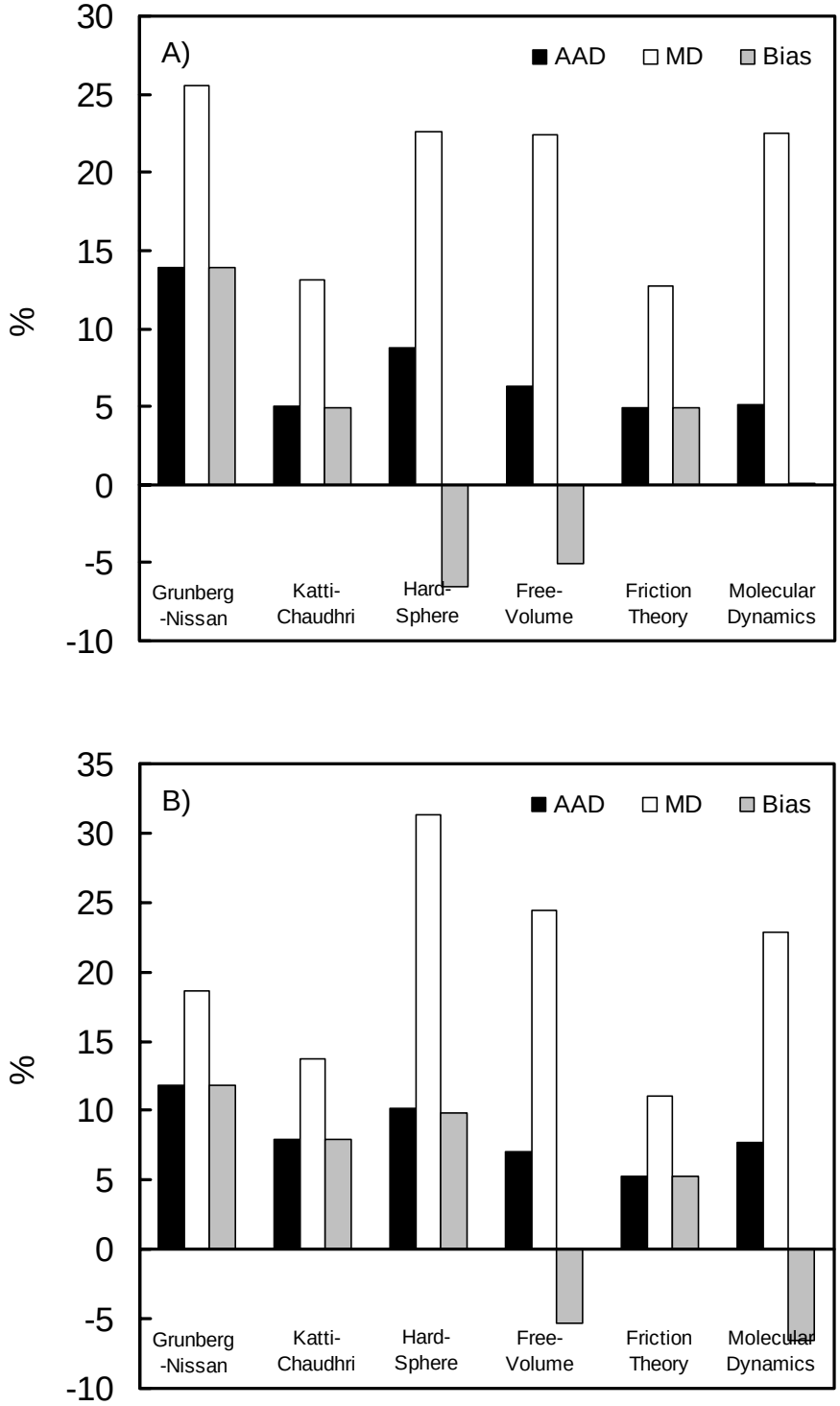
A)
AAD
MD
Bias
%
30
25
20
15
10
5
0
-5
-10
Grunberg -Nissan
Katti-Chaudhri
Hard-Sphere
Free-Volume
Friction Theory
Molecular Dynamics
B)
AAD
MD
Bias
%
35
30
25
20
15
10
5
0
-5
-10
Grunberg -Nissan
Katti-Chaudhri
Hard-Sphere
Free-Volume
Friction Theory
Molecular Dynamics

Figure 7.

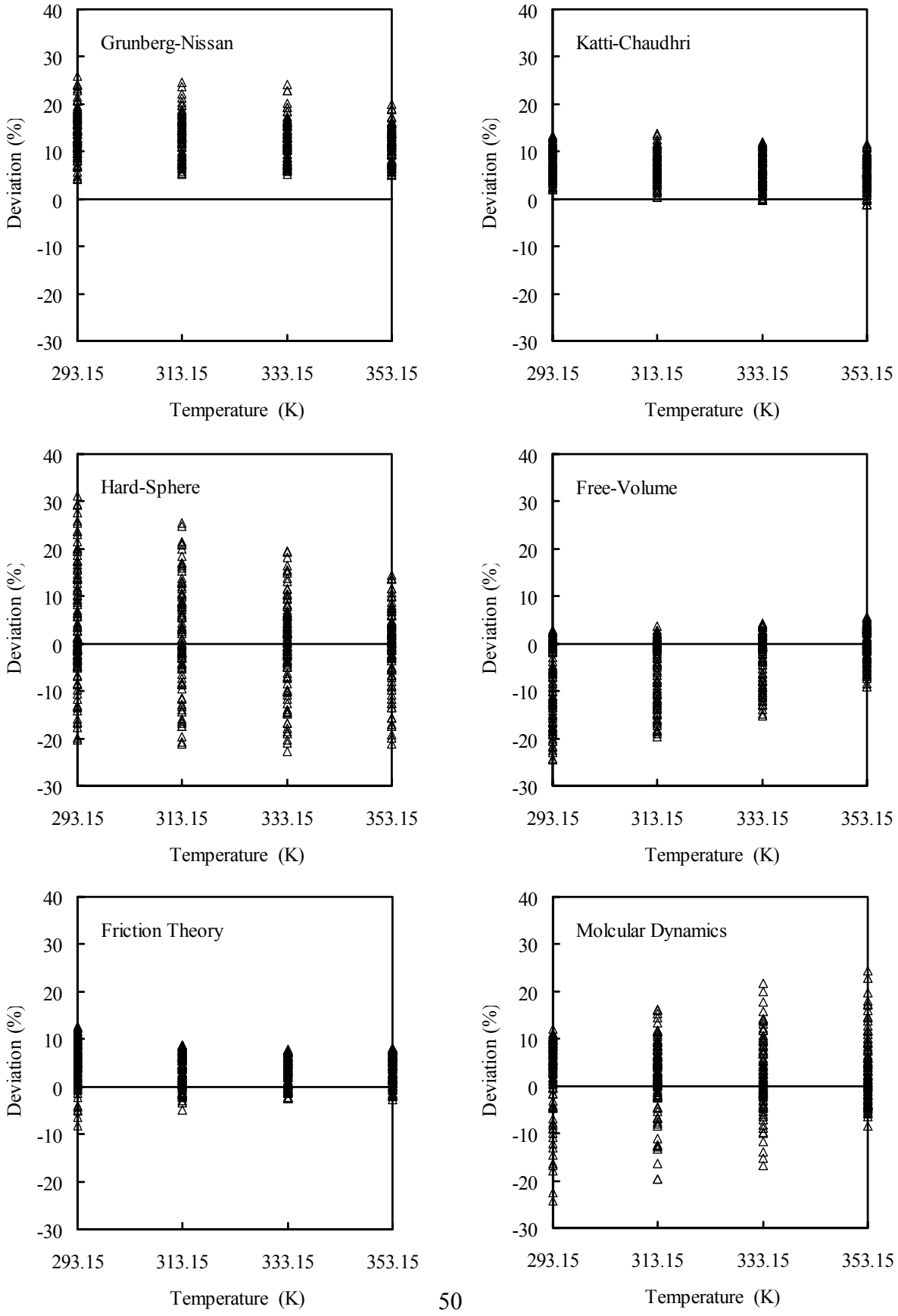
Grunberg-Nissan
Katti-Chaudhri
Hard-Sphere
Free-Volume
Friction Theory
Molcular Dynamics
Deviation (%)
Temperature (K)
40
30
20
10
0
-10
-20
-30
293.15
313.15
333.15
353.15

Figure 8.

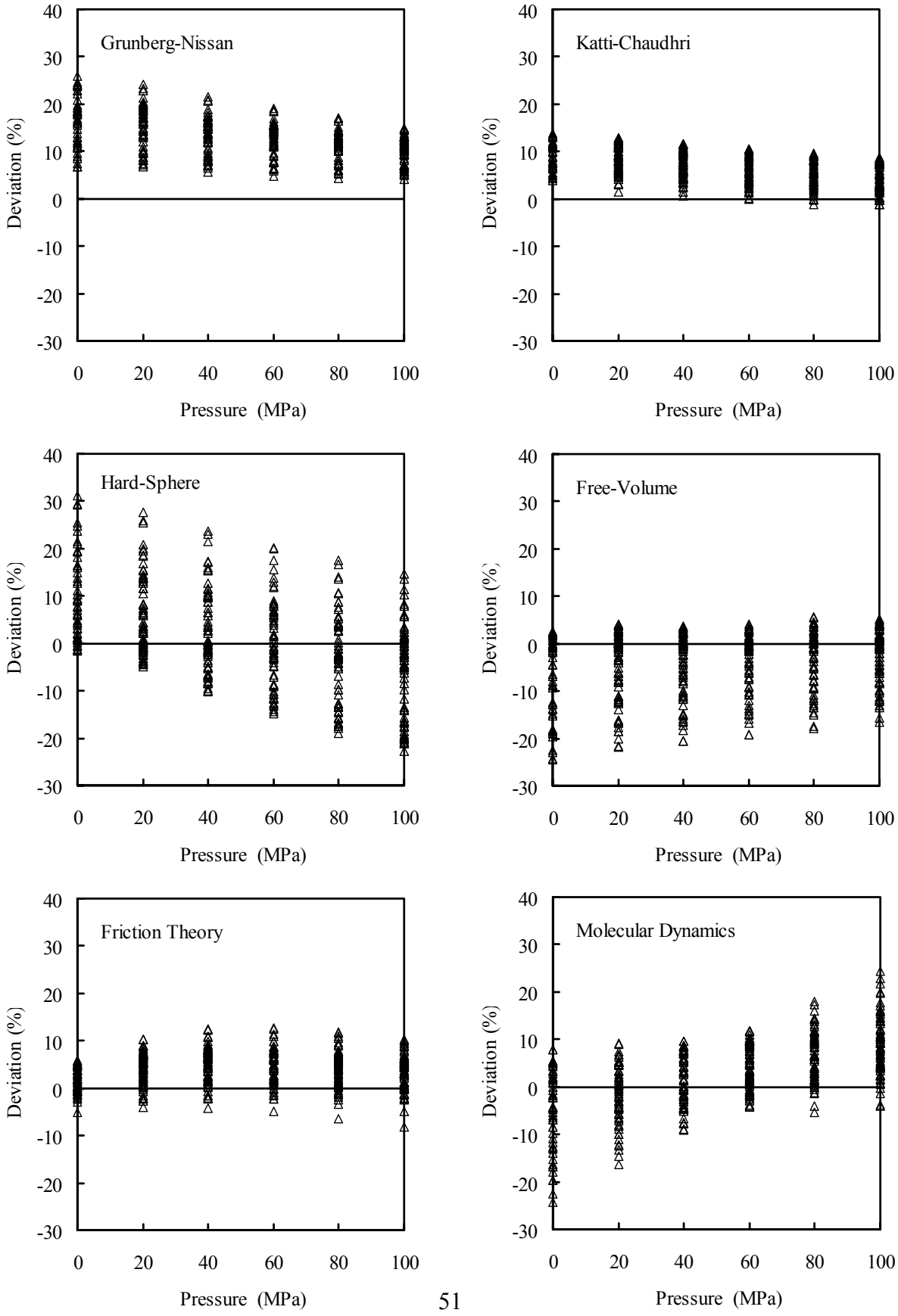
Grunberg-Nissan
Katti-Chaudhri
Hard-Sphere
Free-Volume
Friction Theory
Molecular Dynamics
Deviation (%)
Pressure (MPa)
40
30
20
10
0
-10
-20
-30
0
20
40
60
80
100

Figure Captions

Figure 1. Vapor-liquid phase diagram for ethanol (1) + n-heptane (2) at 0.1 MPa. Experimental data from (○) van Ness et al. [18], (Δ) Wang et al. [19], (×) Ortega and Espiau [20], and (——) predicted by PC-SAFT with $k_{ij} = 0.0435$.

Figure 2. Comparison of dynamic viscosities for n-heptane versus the temperature up to 100 MPa, shown as the deviation, (η_c/η_e-1), between the average fitted values, η_c, obtained from all data (this work and literature [15,23-29] and the experimental values, η_e,: (+) this work, (□) Pensado et al. [15], (○) Agaev and Golubev [23], (◊) Kuss and Pollmann [24], (Δ) Kashiwagi and Makita [25], (×) Assael and Papadaki [26], (•) Kanti et al. [27], (—) Assael et al. [28], (∗) Baylaucq et al. [29].

Figure 3. Dynamic viscosity η for ethanol (1) + n-heptane (2) versus the molar fraction x_1 at T = 293.15 K for (Δ) 0.1 MPa, (×) 20 MPa, (●) 40 MPa, (□) 60 MPa, (○) 80 MPa, and (+) 100 MPa.

Figure 4. Dynamic viscosity η for ethanol (1) + n-heptane (2) versus the molar fraction x_1 at T = 333.15 K for (Δ) 0.1 MPa, (×) 20 MPa, (●) 40 MPa, (□) 60 MPa, (○) 80 MPa, and (+) 100 MPa.

Figure 5. Excess activation energy for viscous flow ΔE_a for ethanol (1) + n-heptane (2) versus the mol fraction x_1 at T = 313.15 K for (Δ) 0.1 MPa, (×) 20 MPa, (●) 40 MPa, (□) 60 MPa, (○) 80 MPa, and (+) 100 MPa.

Figure 6. Deviations, (η_c/η_e-1), between calculated viscosities, η_c, and experimental values, η_e obtained by different viscosity models. A) ethanol + n-heptane and B) ethanol + toluene.

Figure 7. Performance of different viscosity models shown as the deviation, (η_c/η_e-1), between calculated viscosities , η_c, and experimental values, η_e, versus the temperature T at all *T,P,x* conditions for the binary systems ethanol + n-heptane and ethanol + toluene.

Figure 8. Performance of different viscosity models shown as the deviation, (η_c/η_e-1), between calculated viscosities , η_c, and experimental values, η_e, versus the pressure P at all *T,P,x* conditions for the binary systems ethanol + n-heptane and ethanol + toluene.